Electrical resistivity of aluminum below 4.2 K

J. H. J. M. Ribot,* J. Bass,† H. van Kempen, R. J. M. van Vucht, and P. Wyder
Research Institute for Materials, University of Nijmegen, Toernooiveld, Nijmegen, The Netherlands
(Received 18 July 1980)

The resistivities of aluminum samples having resistance ratios ranging from 245 to 40 600 have been measured from 4.2 K down to the superconducting transition temperature $T_c = 1.18$ K. No simple power law could describe the resistivity over this entire temperature range. In the vicinity of 4.2 K, the temperature-dependent portion of the resistivity $\rho(c,T)$ varied approximately as T^3. As the temperature was lowered, it approached a T^2 variation. Below 2.2 K the data were consistent with the form $\rho(c,T) = AT^2 + BT^5$, with A in the vicinity of $2.8\times10^{-15}\,\Omega$ m/K^2 and B in the vicinity of $5\times10^{-17}\,\Omega$ m/K^5. This is the form predicted for a combination of electron-electron and electron-phonon scattering in Al in this temperature range, and the magnitude of B is compatible with calculations for the electron-phonon component. Moreover, the coefficient A was nearly independent of residual resistivity, grain size, dislocation density, sample thickness, and various other parameters tested, exactly as expected if it is associated with electron-electron scattering. On the other hand, the magnitude of A is about 20 times larger than predicted for electron-electron scattering due to screened Coulomb repulsion, and also larger than expected on the basis of radio-frequency size effect and high-temperature Wiedemann-Franz ratio measurements on Al. The most likely resolution of these apparent contradictions lies in the importance of a phonon-mediated electron-electron attraction just above T_c, which MacDonald has recently argued increases the estimated magnitude of A by about a factor of 20 at low temperatures but leaves it unchanged at high temperatures. Finally, the question of "saturation" in the magnitude of $\rho(c,T)$ as the residual resistivity $\rho_0(c)$ is increased, was investigated at both 1.87 K and 4.2 K. At 1.87 K saturation was clearly observed, in that the magnitude of $\rho(c,1.87\text{ K})$ was the same to within experimental uncertainty for all of the samples studied. At 4.2 K, the data for all of the samples given a standard hydrogen anneal were consistent with saturation, but data for samples subjected to other treatments were not.

I. INTRODUCTION

Aluminum (Al) is often chosen to test current theories of electrical transport properties because it is a simple metal for which the electrons can be treated as a nearly free gas.[1] Moreover, it is metallurgically relatively easy to handle[2] and can be obtained in very high purity. On the basis of these characteristics, one might expect that different experiments would agree concerning the variations with temperature and impurity content of a quantity such as the low-temperature electrical resistivity $\rho_t(T)$ of Al (which is measurable in a straightforward fashion) and that the results would be in reasonable accord with calculations.

On the contrary, for nearly a decade there has been controversy concerning: (1) whether below 4.2 K the temperature-dependent resistivity of Al, $\rho(c,T) = \rho_t(T) - \rho_0(c)$, varies more nearly as T^2 or as T^3, (2) whether this resistivity is dominated by electron-electron or electron-phonon scattering, and (3) whether or not $\rho(c,T)$ becomes independent of the residual resistivity $\rho_0(c)$ when the impurity concentration c is increased until $\rho_0(c)$ becomes much larger than $\rho(c,T)$.

The major experimental problem, which results from the high Debye temperature of Al ($\Theta_D \cong 425$ K),[3] is the fact that for even the purest available samples, $\rho(c,T)$ is only a small fraction of ρ_0 below 4.2 K. This means that very-high-precision measurements are needed to resolve small changes in $\rho(c,T)$, and a smooth and accurate temperature scale is needed to ascertain reliably its temperature dependence.

In this paper we present measurements of $\rho(c,T)$ for Al between 4.2 K and its superconducting transition temperature of $T_c = 1.18$ K. These measurements have been made using new technology to obtain higher measuring precision than previously possible, and taking special care to measure temperatures with an accuracy which we believe is better than previously attained in similar studies of Al. These two advantages allow clarification of some experimental points which have been at issue.

The paper is organized as follows. Section II contains a review of previous work on the low-temperature resistivity of Al, both experimental and theoretical, in order to indicate the motivation for the present measurements. In Sec. III, technical details of the measurements are discussed, including sample preparation, measuring technique and procedure, and temperature determination. In Sec. IV the data are presented and analyzed. Section V contains a summary and our conclusions.

II. REVIEW OF PREVIOUS WORK

A. The temperature dependence of $\rho(c,T)$

Modern work on the very-low-temperature resistivity of Al began in the late 1960's with re-

ports by Willot[4] and Panova *et al.*[5] that the resistivity of high-purity Al varied approximately as T^3 below 4.2 K, and a conflicting report by Garland and Bowers[6] that it varied as T^2. The latter two authors tentatively attributed their results to electron-electron scattering in Al, which they described by the relation

$$\rho_{e\text{-}e} = AT^2 \cong 5T^2 \times 10^{-15}\ \Omega\text{m}. \quad (1)$$

These last measurements led Lawrence and Wilkins (LW) to examine theoretically the low-temperature resistivities to be expected for Al due to electron-electron (e-e) and electron-phonon (e-ph) scattering.[7,8] Since below 4 K the resistivity of Al is dominated by impurity scattering, which is expected to be nearly isotropic in k space, they used a trial electronic distribution function appropriate to such scattering. Their calculations are thus representative of what is euphemistically called the "dirty limit" in Al. To make the calculations tractable, they considered only electronic states which could be described by one or two orthogonalized-plane-wave (1- or 2-OPW) states. They thus neglected effects of the small number of 3- and 4-OPW states on the Fermi surface of Al. At the lowest temperatures this neglect probably introduces into their estimate of the magnitude of the electron-phonon resistivity an uncertainty of at least a factor of two.

LW treated electron-electron scattering in terms of a Thomas-Fermi screened Coulomb interaction. In the dirty limit they calculated

$$\rho_{e\text{-}e}^{\text{calc}} = 0.12T^2 \times 10^{-15}\ \Omega\text{m} \quad (2)$$

with little change expected as the sample became purer. The anticipated uncertainty here is also about a factor of 2 or 3. Since this estimate was 40 times smaller than the T^2 term deduced by Garland and Bowers, they concluded that the resistivity seen by Garland and Bowers could not be due to electron-electron scattering.

For electron-phonon scattering in the dirty limit, LW found a T^5 variation below about 3 K,[8] with a coefficient which we estimate (by extrapolating their published curve to lower temperature) to be

$$\rho_{e\text{-}ph}^{\text{calc}} \cong 20T^5 \times 10^{-17}\ \Omega\text{m}. \quad (3)$$

Above 3 K, their $\rho_{e\text{-}ph}$ increased more slowly than T^5, varying approximately as T^4 from 4 K up to 10 K. In this temperature range, their calculated $\rho_{e\text{-}ph}$ was larger than the experimental $\rho(c, T)$, but decreased toward it as T approached 3 K.

If we compare Eqs. (2) and (3), we see that Lawrence and Wilkins predict that $\rho_{e\text{-}ph}$ should dominate $\rho_{e\text{-}e}$ at all temperatures for which Al is not a superconductor, leading to an approximately T^5 variation for the dirty limit of $\rho(c, T)$ between 4.2 and 1.18 K. This prediction disagrees with both the T^2 and T^3 variations actually reported. In 1973, Senoussi and Campbell[9] re-examined $\rho(c, T)$ below 4 K for three relatively impure Al samples and found a T^3 variation, a result which was supported soon afterwards by measurements of Babić *et al.*[10]

Kaveh and Wiser[11] proposed an explanation for the data of Senoussi and Campbell in terms of a combination of electron-electron and electron-phonon scattering. They showed that if they subtracted from these data their own calculated values of $\rho_{e\text{-}ph}$ for Al (which were about half as large as Lawrence and Wilkins's values), then the resistivity which resulted was

$$\rho_r = (2.1 - 2.6)T^2 \times 10^{-15}\ \Omega\text{m}. \quad (4)$$

This was of the same form as claimed by Garland and Bowers for the total resistivity but only about half the magnitude. Kaveh and Wiser attributed the T^2 term of Eq. (4) to electron-electron scattering and ascribed Lawrence and Wilkins's failure to obtain such a large value to difficulties in properly treating electron screening, arguing that the magnitude of the T^2 coefficient is very sensitive to the screening length.

Soon afterward, Gasparov and Harutunian[12] looked for independent evidence of electron-electron scattering by measuring the radio-frequency size effect (RFSE) in Al from 10 K down to about 2 K. According to simple theory, electron-electron scattering should appear in the RFSE as a T^2 term, while electron-phonon scattering should appear as T^3. To within experimental uncertainty, their data were consistent with a T^3 variation over the temperature range studied, a result consistent with the relatively small amount of electron-electron scattering estimated by Lawrence and Wilkins.

Stimulated by the above-mentioned claims of T^3 resistivities in Al below 4 K, and by the lack of evidence for electron-electron scattering from the RFSE measurements, Garland and van Harlingen[13] measured the electrical resistivities, the thermal resitivities times temperature, and the thermoelectric coefficients of several high-purity Al samples below 4.2 K. They reported finding T^2 variations for all three quantities, with magnitudes of the electrical resistivities that agreed with the older results of Garland and Bowers.

As indicated above, these conflicting claims led us to also measure the resistivities of Al samples of varying purity, in the hope that higher measuring precision combined with special care in temperature determination would allow us to resolve some of these experimental discrepancies. A portion of our results have been described in two

short communications[14] in which we argued in favor of a combination of electron-electron and electron-phonon scattering in the resistivity of Al below 4 K, with an electron-electron component comparable to that proposed by Kaveh and Wiser.[11]

Since the appearance of these two communications, there have been some important additional developments. First, it was pointed out to us[15] that published Wiedemann-Franz ratio data for Al at high temperatures could be interpreted as conflicting with an electron-electron resistivity component as large as we were proposing. Analysis of Wiedemann-Franz ratio data suffers from difficulties resulting from the small contribution that electron-electron scattering makes to the quantities measured, as well as from limitations on the precision and accuracy of the measurements and on our understanding of the corrections to be made for higher-order electron-phonon scattering effects at high temperatures. Nonetheless, the most straightforward analysis of the existing data does tend to support the Lawrence and Wilkins calculation and the Gasparov and Harutunian RFSE data in opposition to our interpretation. Second, very recent RFSE measurements on Al by Parsons and Steele[16] have yielded data that seem to vary more nearly as $T^{2.5}$ than as T^3. These results raise some question concerning the simple T^3 variation reported by Gasparov and Harutunian, and thereby weaken the RFSE argument against electron-electron scattering. And finally, very recent theoretical developments which we will describe below, both increase the estimated magnitude of the electron-electron scattering coefficient toward the value we suggest and provide a possible explanation for differences between high- and low-temperature coefficients.

We see from this discussion that there is considerable disagreement in the literature concerning both the temperature dependence and the source of the low-temperature resistivity of Al. In an attempt to establish the limits of what we know and what we do not, we shall describe in this paper all of the results which we have obtained, including some measured since the publications of the two previous communications, and examine in detail various possible alternative interpretations of the data, taking into account all of the available evidence.

B. The variation of $\rho(c,T)$ with ρ_0

According to the usual "isotropization" or "generalized two-band" model of deviations from Matthiessen's rule in the limit where impurity scattering of electrons dominates over phonon scattering (dirty limit), the temperature-dependent resistivity of a dilute alloy should become independent of the residual resistivity $\rho_0(c)$.[17,18] This process is referred to as "saturation" into the dirty limit, in the sense that the resistivity reaches a maximum value (saturates in magnitude) after which it remains constant as $\rho_0(c)$ increases further.

At higher temperatures ($T \geq 14$ K) where quite a bit of data exists for Al, saturation has not been found.[10] This lack of saturation may be due to three causes. Firstly, when the impurity concentration becomes large, higher-order resistivity components involving a combination of electron-phonon and electron-impurity scattering, begin to become significant. These components vary with ρ_0 and thus do not saturate as ρ_0 becomes large. Nonsaturation in Al at 14 K and above has been attributed to the appearance of such components.[19] Secondly, the highest values of ρ_0 measured were obtained with samples which had been rapidly quenched in an attempt to keep impurities in solution to well above their normal solubility limit.[10] It is thus not completely clear that these samples satisfied all of the various conditions (such as random distribution of impurities) needed for the simple model which predicts saturation to be valid. Thirdly, there may be an additional mechanism, not yet understood, which produces the nonsaturation. It is this third alternative which we wished to investigate.

This could be done by going to much lower temperatures ($T \leq 4.2$ K), where the impurity concentration needed to reach the dirty limit is greatly reduced, thereby eliminating the first two alternatives described above. If saturation is then observed, no additional mechanism is needed for the higher-temperature data.

To date, no single experimenter has investigated the question of saturation in Al at or below 4.2 K using a series of samples of widely varying purity. Senoussi and Campbell[9] combined data from several sources to obtain evidence of approximate saturation at 4.2 K. However, the scatter in the data was so large that nonsaturation could also be inferred. We thus decided to investigate whether $\rho(c, T)$ saturates in Al at 4.2 K and below, and the results of this investigation will also be described.

III. TECHNICAL DETAILS

A. Sample preparation and characterization

Measurements were performed on 12 Al samples with residual resistance ratios, RRR $\equiv R(300\text{ K})/R(1.2\text{ K})$, ranging from 245 to 40 600 (see Table I).

(1) The four purest samples (nr. 1–4) were cylindrical wires about 1.5 m long, wound in a

double helix around a quartz cylinder. The diameter and length of the helix were both about 40 mm. Before mounting, the samples were cleaned in a 40% NaOH solution. This facilitated the spotwelding to the samples of 1-mm diameter ultrapure Al wires as potential leads. These leads were several cm long and were attached at least 10 wire diameters in from the ends of the sample. The welds were made with the minimum electrical energy needed to achieve mechanical stability and showed no extra oxide formation. After annealing, a test weld had a resistance of less than 5×10^{-8} Ω at 4.2 K. Once the potential leads were attached, the samples were annealed in dry hydrogen ($\leq$10 ppm $\times H_2O$) at one-atmosphere pressure for 1 h at 773 K and 1 h at 673 K, after which they were cooled slowly to room temperature over a period of about 10 h. A given sample was then mounted in the measuring system, and superconducting current and potential wires were attached to it using superconducting solder containing Pb, Sn, and Ag.[20]

(2) The four lowest-purity samples (nr. 5, 6, 10, and 11) were straight, cylindrical wires about 10 cm long. Samples 5, 6, and 10, were cleaned in the NaOH solution, annealed in hydrogen as described above, and then recleaned in the solution. Ultrapure, 3 cm long, Al potential leads were then spotwelded to each sample about 2 cm in from each end. The sample was then mounted and the current and potential leads attached with solder as described above. Sample 11 was taken from the same roll as sample 5 and prepared in the same way, except that it was annealed in air to see what effect this would have on the total increase in resistiv-

TABLE I. Sample characteristics and main results.

Sample	Diam. (mm)	ρ_0 (10^{-12} Ωm)	RRR	Nominal impurity (ppm)
1	1.4	0.928	29.000	<0.5
2	3.0	0.667	40.600	<0.5
3	3.0	1.30	21.000	< 5
4	3.0	2.92	9.300	< 8
5	2.0	106.8	255	<100
6	1.0	110.6	245	unknown
7	1.0[a]	6.63	4.100	<10
8	1.0[a]	6.01	4.500	<10
8b	1.0[a]	6.33	4.300	<10
9	1.0[a]	22.45	1.100	<10
10	2.0[a]	31.56	860	unknown
11	2.0	104.1	260	<100
12	1.0[a]	7.26	3.700	<10
12b	1.0[a]	7.26	3.700	<10

	Grain size (mm)	Relative accuracy (ppm)	A (10^{-15} ΩmK^{-2})	B (10^{-15} ΩmK^{-5})	$\rho(c, 4.2\ \mathrm{K})$ (10^{-14} Ωm)
1		3	2.8 ± 0.1	$0.04^5 \pm 0.01$	8.6
2	5	4	2.7 ± 0.1^5	0.05	8.5
3		2	$2.9^5 \pm 0.1^5$	0.05	9.6
4	1.5	1	$2.8^5 \pm 0.2$	0.06	10.5
5	0.2	2	$3.0^5 \pm 0.4$		11.9
6	0.25	1	$3.0^5 \pm 0.3$		12.1
7	1	2	2.7 ± 0.1^5		9.5
8	1	2.5	2.7 ± 0.1^5		9.4
8b		2.5	2.7 ± 0.2^5		8.7
9	$\leq$0.2	1.5	$3.0^5 \pm 0.3$		9.6
10		2	not measured		11.6
11		2	not measured		12.5
12		2.5	2.9 ± 0.3		11.5
12b		2.5	2.9 ± 0.2		11.3

[a] Approximately square samples (number given is width).

ity of a low-purity sample between 0 and 4.2 K.

(3) Four samples of intermediate purity (nr. 7–9 and 12) were used to check for possible effects of sample geometry, spot-welding, and annealing atmosphere on both the lowest-temperature and higher-temperature resistivities. These samples were all spark cut from a single Al sheet of 1 mm thickness. Each sample was approximately 10 cm long, 1 mm wide, and contained four tabs, 1 mm wide and 2 mm long, located approximately symmetrically on the sample about 1 cm in from each end. After spark-cutting, the samples were cleaned in the NaOH solution. The annealing procedures for the samples were as follows. Sample 7 was annealed in air following the recipe outlined above. Sample 9 was left unannealed. Sample 8 was annealed in hydrogen for 22 h. After measurement and subsequent etching to check grain size, sample 8 (now relabeled 8b) was again annealed in hydrogen at the same time as sample 12. These two samples were apparently accidentally heated above 773 K, as inferred from the fact that both sagged badly during the anneal. After annealing, each of the above samples was mounted and current contacts were soldered to its ends. For samples 7, 8, and 9 the potential contacts were soldered to the ends of two tabs on the same side of the sample. For sample 12 a 4-cm long, pure-Al potential lead was spot welded to each tab before the sample was annealed. After annealing, the potential contacts were soldered to those leads. After sample 12 was measured, the Al leads were removed, giving sample 12b, to which the potential contacts were then soldered in the same way as for samples 7–9. Sample 12b was measured with no further annealing.

After they were measured, seven of the twelve samples were etched to determine typical grain sizes along the sample length. The values obtained are listed in Table I. In each case examined, the grain size was larger than the estimated electron mean-free path at 4.2 K.

The geometrical factor (length divided by cross-sectional area) was determined for each sample with a precision of 0.1% by measuring the resistance at room temperature, T_r, and assuming a resistivity of $\rho(T_r) = 24.28 + 0.113T_r$ nΩm,[21] where T_r is measured in degrees Celsius. The geometrical factors determined in this way were equal to the directly measured lengths divided by the cross-sectional areas to within the measuring error of $\leq 3\%$. No corrections have been made for sample contraction ($0.37 \pm 0.02\%$) (Ref. 21) between room temperature and liquid helium.

B. Electrical measurements

The resistances of the samples at helium temperatures were measured with a bridge circuit, immersed in the liquid helium, that consisted of the sample R_1, a comparison resistor R_2, and a superconducting flux-gated galvanometer. The galvanometer was used as a null detector in a feedback system which regulated the ratio of the two currents I_1 and I_2 going through R_1 and R_2, respectively. The two currents were delivered by a current comparator which under optimal conditions provided a precision in I_1/I_2 of 0.1 parts per million (ppm). The entire electrical-measurement system is described in detail in Ref. 22.

At helium temperatures, the achieved precision in I_1/I_2 (and thus in R_1) was limited by the sensitivity of the flux-gated galvanometer. It thus depended upon both the magnitude of the current used and the ratio R_1/R_2. The maximum current through a sample was always chosen to be either 0.3 A or whatever lesser value was necessary to keep the current through the reference resistor below 1 A, since the reference resistors had been found to be current independent for currents up to 1 A.[22] The achieved relative precision in the measurement of R_1 is defined as the ratio of the smallest reliable digit to the total value of R_1, using the largest measuring current employed with the given sample. The resulting values are given for each sample in Table I. These values indicate the random uncertainties in a single measurement of R_1 resulting from the electrical measuring process alone. Above T_λ, temperature fluctuations made this precision unattainable. Below T_λ it could sometimes be improved upon by making multiple measurements of the same quantity.

For several samples, different currents were used to check that the inferred resistances were independent of the magnitude of the current. An example of the results obtained is shown in Fig. 1 which shows for sample 4 the values of $\Delta\rho/T\Delta T$ obtained with measuring currents of 0.3 A (crosses) and 0.07 A (open circles). As illustrated there, no current dependence of R_1 ($d\rho_1/dI < 3 \times 10^{-16}$ Ωm/A, was ever found to within the achieved relative precision for the smaller current used (i.e., to within the value listed in Table I multiplied by the ratio of the larger current to the smaller).

For sample 2, the transition through T_c was measured to see if the magnetic field of the current and the earth's magnetic field produced any

unexpected effects. The data are shown in Fig. 2. The observed shift in transition temperature and the broadening of the transition are in accordance with the calculated variation of the resultant magnetic field over the sample (between 0 and $10^{-4}T$ for this sample). A decrease of 56 K/T in the transition temperature was assumed.[23] To minimize effects of the earth's magnetic field, the measurements on samples 4–9 were made with the samples enclosed in a Pb shield surrounded by a sheet of μ metal.

Following a report[24] of a large temperature dependence in $\rho(T)$ for Al below 2 K using current densities of less than 1 A/cm^2, we looked for such an effect in both the high-purity sample 3 and the low-purity samples 5 and 6. No such effect was observed, and the report was subsequently attributed by its authors to difficulties with soldered potential leads.[25] We have not checked a much smaller reported effect occurring only in still-lower-purity samples.[25]

Aside from uncertainties associated with temperature determination, which will be dealt with in the next section, the only other source of uncertainty in R_1 is the uncertainty in the temperature dependence of R_2. Sample 1 was measured against a comparison resistor of commercial copper with beryllium which had $(1/R)(dR/dT) \approx -2 \times 10^{-4}$ K^{-1}. The other samples were measured against a resistor made of copper with 5% phosphorus[26] which had $(1/R)(dR/dT) \approx -10^{-5}$ K^{-1}. The variation with temperature of each of these resistors was determined by comparison with an as-nearly-identical-as-possible resistor held at a constant temperature of 4.2 K. For the copper-beryllium resistor, the corrections for temperature dependence were uncertain to about ±2 ppm. For the copper-phosphorus resistor, the scatter in the data about a smooth curve was approximately ±1 ppm from 4.2 down to 1.5 K. Below 1.5 K, only a single point was taken, at 1.25 K; this point fell below the continuation of the smooth curve by about 2 ppm. These uncertainties become significant only for the three or four least-pure samples at the lowest temperatures.

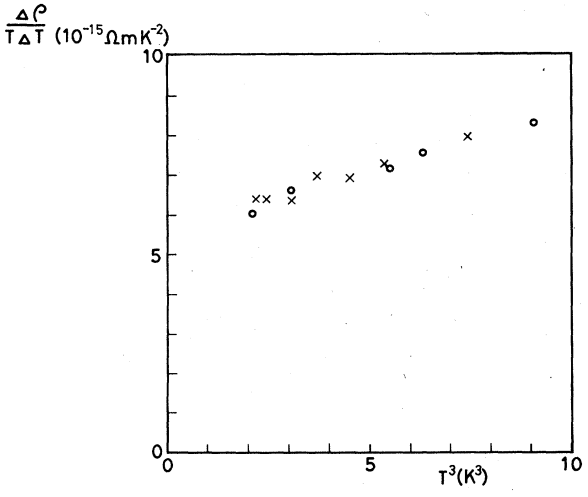

FIG. 1. $\Delta\rho/T\Delta T$ vs T^3 for sample 4, measured with two different currents: the crosses were measured with a current of 0.3 A, the open circles with 0.07 A.

C. Temperatue determination

Temperatures were determined by measuring the vapor pressure of the ^{4}He bath in which the sample was immersed, and using the temperature scale T_{58}.[27] The bath was connected to the pressure meters by a stainless-steel tube of 6-mm diameter which extended to just above the bath level. The pressure meters were quartz tube manometers,[28] one which was 0–100 Torr and the other, one 0–1000 Torr, with resolutions of 0.0005 and 0.005 Torr, respectively. The pressure meters were corrected for the following: (1) Zero offset – checked during each measuring run, (2) calibration and oven-temperature corrections as supplied by the manufacturer of the manometers, (3) the pressure at the reference side of the differential manometers usually about 25 mTorr, as measured with a thermocouple gauge, (4) above T_λ, the pressure head correction[27] (near

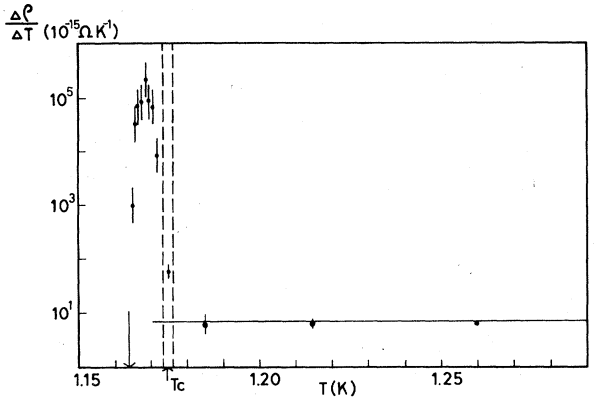

FIG. 2. The derivative of the resistivity $\Delta\rho/\Delta T$ vs T for sample 2 around the superconducting transition temperature. T_c indicates the transition temperature of the Al in an NBS temperature calibration device in zero magnetic field; the dashed lines indicate the breadth of the expected transition for zero field. The broadening and shift of the measured transition of sample 2 can be explained by effects due to a combination of the self-magnetic field due to the current in the sample plus the earth's magnetic field. The solid line gives a fit to $\rho(T) = AT^2 + BT^5$ between 1.2 and 2.2 K.

T_λ this caused the biggest error in the temperature determination by this method), and (5) below 1.5 K a thermomolecular pressure correction[29] as determined by calibration of the superconducting transition temperature T_c for aluminum (see below).

The accuracies of the vapor-pressure temperatures were checked with two secondary thermometers, one a ^{3}He vapor-pressure bulb immersed in the liquid ^{4}He (used only below T_λ), and the other a factory calibrated germanium thermometer[30] (used above 1.5 K). In addition, the temperature scale was specifically tested at three standard calibration points, one at the lower end, one in the middle, and one at the higher end; namely, by measuring the T_c's of Al and In (Ref. 31) and by measuring T_λ. The results of these calibrations and cross checks are summarized in Figs. 3–5.

Figure 3 shows the pressure p_λ of T_λ as measured over a period of years using the manometers. The average value $p_\lambda = 37.83 \pm 0.01$ Torr corresponds to a temperature difference of only 0.3 mK from the T_{58} value of 37.80 Torr. This difference is so small that no correction has been made for it.

Figure 4 shows a comparison between the temperature T_{He} as determined from the vapor pressure of ^{4}He (T_{58} scale) and the temperature T_{Ge} determined with the factory-calibrated germanium thermometer. This thermometer was calibrated against T_{62} at 2 K and below, and against $T_{NBS2\text{-}20}$ (Ref. 32) above 2 K. Because of the 6-mK difference[33,34] between T_{62} and $T_{NBS2\text{-}20}$ around 2 K, quite large discontinuities can be expected in thermometers calibrated in this way, as can be seen in Fig. 4.

The data of Fig. 4 were used to convert measured values of T_{Ge} into equivalent values of T_{He}. T_{Ge} was always measured along with T_{He}, both to serve as a check that no systematic errors were creeping into T_{He} over time, and to provide data with less scatter between 3 K and T_λ (see below).

Figure 5 shows three things:

(1) First, the difference between the ^{4}He and the ^{3}He temperature determinations. These differences, indicated by crosses between 1.2 K and T_λ corresponded to about 1.5 mK, and are attributed primarily to a combination of radiation heat input via the tube attached to the copper bulb containing the ^{3}He, and to a too-high Kapitza resistance between the bulb and the ^{4}He bath due to inadequate size of the copper fins used in an attempt to equilibrate the bulb to the bath. In any case, the difference of 1.5 mK is comparable to our claimed uncertainty.

(2) Second, the differences between T_{58} and our three calibration points (dots on the graph). The middle dot, corresponding to T_λ, has already been discussed. The higher-temperature dot corresponds to T_c for indium, for which we measured 318.10 ± 0.05 Torr. This is within the uncertainty of the $T_{NBS2\text{-}20}$ value of 318.26 ± 0.8 Torr, which corresponds to a value of 3.409 ± 0.002 K (Ref. 31) (Ref. 34 gives 3.407_7 K). Finally, the lowest-temperature dot is intended to indicate the uncertainty of our value of T_c for Al after application of a thermomolecular correction determined as follows. We measured T_c for Al with a National Bureau of Standards Model 767 superconducting thermometric fixed-point device, and after making all of the standard corrections listed above, obtained $T_c = 1.181$ K. The T_c given by the N.B.S.

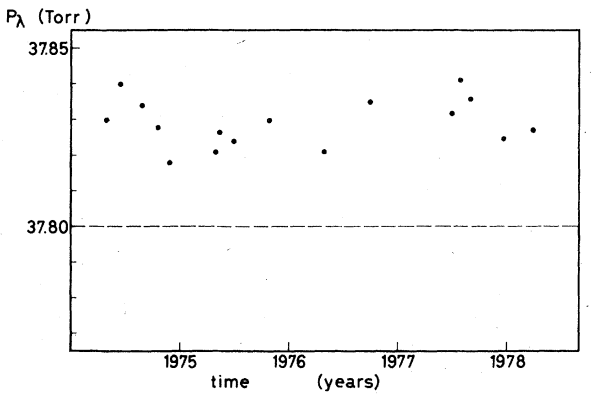

FIG. 3. Measurements of the vapor pressure p of ^{4}He at the superfluid transition temperature. No drift is visible over 4 years. The value given in Ref. 27 is $p_\lambda = 37.80$ Torr.

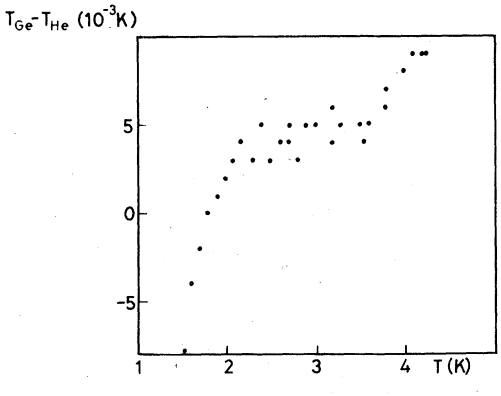

FIG. 4. Comparison between the temperature T_{He} as determined from the vapor pressure of ^{4}He (T_{58} scale) and the temperature T_{Ge} determined with a factory-calibrated germanium thermometer. The scatter above T_λ is typical for the reproducibility obtained between different runs and is caused primarily by the difficulty of determining T_{He}.

(Ref. 31) is $1.174_6 \pm 0.002$ K (Ref. 34 gives 1.176_4 K on the same scale). To bring our value into agreement with the N.B.S. value required subtraction of 25 mTorr from our measured pressure. We thus took this value to be the thermomolecular correction. If instead we used a calculated thermomolecular correction[29] based upon the properties of our pressure line, we found a value of $T_c = 1.175_5$, right in the middle of the two values listed above. The dot at 1.174 K in Fig. 5 indicates the 0.9-mK difference between the values for T_c determined using the calculated and fit corrections.

(3) Third, the graph also shows the scatter in our ^{4}He determinations of T as determined by analyzing differences between temperatures measured using the ^{4}He vapor pressure and the Ge-resistance thermometer, and also by comparing the measured resistances of our samples at different bath levels. The scatter is indicated by the dashed lines. Just above T_λ, the Ge thermometer gave less scatter ($\approx$0.5 mK) than measurements of the ^{4}He vapor pressure; it was therefore usually used as the standard in this temperature region.

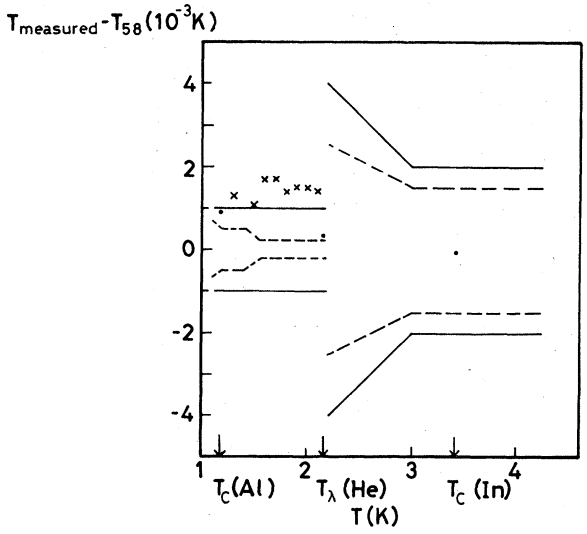

FIG. 5. Checks on the difference between the temperature as determined from the ^{4}He vapor pressure (T_{measured}) and T_{58}. (a) The three dots represent the difference between T_{measured} and official values of some transition temperature expressed on the T_{58} scale. The T_c of aluminum was used to revise a calculated correction term (see text). (b) The crosses represent some typical differences found between T_{measured} and the temperature determined from a ^{3}He vapor-pressure measurement. (c) The solid and interrupted lines give, respectively, the estimated error and scatter in the temperature determination from ^{4}He vapor pressure. Note that the small error at the lowest temperatures is obtained only after using the T_c(Al) to determine the thermomolecular pressure gradient (see text).

From these figures we estimate the uncertainty in T at about ± 2 mK above T_λ and somewhat better below. Because the major errors in T are systematic in nature and slowly varying functions of T, systematic errors in temperature differences are smaller than those in the temperatures themselves; thus inaccuracies in ΔT are due primarily to random and round-off errors. We estimate the uncertainty in ΔT to be less than 1 mK below T_λ and 1–2 mK above.

Finally, we note that all temperatures in this paper are expressed on the T_{58} scale. Calibrations which were expressed on different scales have been corrected to the T_{58} scale as described above. The differences between T_{58} and T_{76} are smooth (see Fig. 6) and too small to significantly affect the data analysis to be presented.

D. Achieved uncertainties

For most of the samples, the scatters achieved in the experimental data and in their derivatives were about as expected from the estimates given above for T, ΔT, and $\Delta\rho$. Thus for the purest samples, in which the uncertainties in ΔT were dominant, the uncertainties in $\Delta\rho/\Delta T$ were usually $\leq 1\%$ when we used values of $\Delta T \geq 0.1$ K below T_λ and $\Delta T \geq 0.2$ K above. As the purity of the samples decreased, $\Delta\rho$ became a smaller fraction of ρ_0 and the uncertainties in $\Delta\rho$ became more important. Thus for the least-pure samples, the uncertainties in $\Delta\rho/\Delta T$ were typically a few percent, even though we used larger values for ΔT. This is the reason for the larger estimated uncertainties in the coefficients A for these samples listed in Table I.

The only exceptions to these remarks (aside from an occasional bad point) occurred in samples 1–4, which, for a variety of reasons were measured over periods of several days to two weeks. During these periods, the samples sometimes

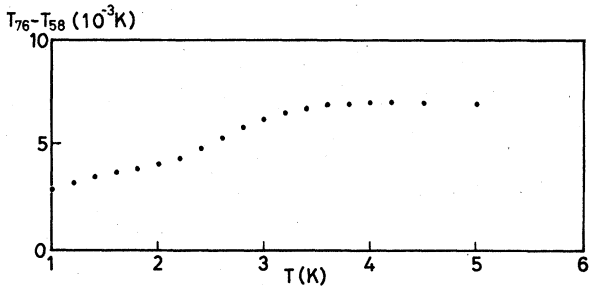

FIG. 6. Comparison (from Ref. 34) between the 1976 provisional temperature scale (T_{76}) and T_{58}.

warmed up to liquid-nitrogen temperature, and in at least one case to room temperature. In the process, small systematic changes occurred in the sample resistances. Multiplicative corrections of order 10^{-4} were made for these changes, using the resistance of the sample at a fixed temperature just below T_λ as a reference. However, these corrections never produced agreements at temperatures other than T_λ as good as those obtained during individual measuring runs. For this reason, we recommend that for highest accuracy, derivatives be calculated for these samples using only data points taken during the same run, and we have adopted this procedure in the present paper. The procedure is important primarily for samples 3 and 4. In the Appendix, where the resistivities of our samples are given, we have labeled by the same letter those data points which were taken together.

IV. EXPERIMENTAL RESULTS AND DATA ANALYSIS

We investigate in this section how the resistivities of our samples vary with temperature, and also how they vary from sample to sample at fixed temperatures. The section is organized as follows. In part A we describe how we calculate the temperature derivatives which are used in most of the subsequent analysis. In part B we examine whether $\rho(c, T)$ can be described by any of the simple power laws (T^2, T^3, or T^5) predicted by the theorists or reported by previous investigators; we find that it cannot. In part C *1*, we show that the lowest-temperature data satisfy both of the qualitative criteria traditionally supposed to indicate the presence of electron-electron scattering—namely, a dominant T^2 variation and a magnitude which is independent of $\rho_0(c)$. We show also that a combination of electron-electron and electron-phonon scattering provides an adequate qualitative description of the temperature dependence of $\rho(c, T)$ over the entire temperature range investigated. In part C *2*, however, we find that the magnitude of the electron-electron component of the resistivity inferred in part C *1* is much larger than expected, either from the usual theory involving a screened Coulomb interaction between electrons or from measurements of both the radio-frequency size effect (RFSE) and the high-temperature Wiedemann-Franz ratio of Al. A new calculation[38] based upon phonon-mediated electron-electron scattering, provides a plausible resolution of these discrepancies, but it is not yet clear whether it represents the last word about this complex theoretical subject. It therefore seems worthwhile to investigate whether there are other possible ways to interpret our data. In Sec. IV D we examine whether the source of $\rho(c, T)$ could be something other than electron-electron or electron-phonon scattering. We conclude that it cannot. We finish our analysis of the temperature variation of $\rho(c, T)$ in part E, in which we investigate whether alternative possible forms for the electron-phonon component of the resistivity can lead to a significant reduction in the size of the inferred electron-electron component. In part F we examine the variation of $\rho(c, T)$ with $\rho_0(c)$ for two fixed values of T, namely, 1.87 and 4.20 K, in order to investigate the question of saturation in $\rho(c, T)$ at such low temperatures.

A. Calculation of the temperature derivative of $\rho(c,T)$

Below 1.18 K, Al is a superconductor. This means that its residual resistivity $\rho_0(c)$ cannot be measured by simply going to very low temperature. In order to analyze our data without treating ρ_0 as an adjustable parameter, it must be eliminated from the problem. We did this by calculating the temperature difference of the data:

$$\frac{\Delta\rho}{\Delta T} = \frac{\rho_t(T_2) - \rho_t(T_1)}{T_2 - T_1} \ . \tag{5}$$

To make the calculated differences closely equal to the derivatives of interest, we required for the purer samples that $\Delta T/T \leq 0.1$. This requirement could be satisfied and the scatter in the derivatives still kept acceptably low using $\Delta T \geq 0.1$ K below T_λ and $\Delta T \geq 0.2$ K above T_λ. For the least-pure samples, it was usually necessary to use values at least twice as large as these to keep the scatter acceptable.

B. Search for a simple power-law variation of $\rho(c,T)$ with T

As indicated in Sec. II above, the theorists predict that electron-phonon scattering will dominate electron-electron scattering in Al to below $T_c = 1.18$ K, leading to an approximately T^5 variation of the resistivity between about 3 K and T_c. The experiments, in contrast, have made conflicting claims that the resistivity varies either as T^2 or T^3.

The usual procedure for testing for a simple power-law variation is to plot $\rho(c, T)$ as a function of T^n, the assumed power of T. If the law is obeyed, the data will fall on a straight line. This procedure has two disadvantages. First, for $n \geq 2$ it weights high-temperature data points more heavily than low-temperature ones. Second, it tends to obscure small systematic deviations from power-law behavior, especially at the lowest temperature.

We shall adopt instead an alternative procedure which both weights the data points more nearly equally and makes deviations from power-law behavior visually manifest. The procedure is to plot $(1/T^m)(\Delta\rho/\Delta T)$ as a function of T for various assumed values of the integer m. If $\rho(c,T)$ varies as T^{m+1}, such a plot will yield a horizontal straight line.

Figure 7 shows a plot of $(1/T^m)(\Delta\rho/\Delta T)$ for sample 1, one of our purest samples, using $m = 0$, 1, 2, and 3. For ease of comparison of the different curves, the quantities of interest have all been normalized to the value 1.00 at the highest temperature shown. We see immediately that none of the curves are flat over any significant portion of the temperature range. This means that for this sample $\rho(c,T)$ does not vary as T^{m+1} for any integer value of m, either over the entire temperature range or over any substantial portion of it. Instead, its variation falls between T^2 and T^3, approaching nearer to T^3 at higher temperatures and to T^2 at lower ones.

To examine whether the qualitative behavior shown in Fig. 7 is independent of sample purity, we compare in Fig. 8 the behavior of $(1/T^m)(\Delta\rho/\Delta T)$ for the high-purity sample 1 with the behavior of the same quantity for a sample of intermediate purity (sample 4) and for one of low purity (sample 6). For simplicity, attention is restricted to the values $m = 1$ and 2 which bracketed the data of sample 1 in Fig. 7. We see from this figure that at the lowest temperatures all three samples approach a T^2 variation in very much the same way. However, at higher temperatures there are slight systematic differences between their forms: Sample 1 always varies more slowly than T^3, sample 4 varies very nearly as T^3 over most of the temperature range, showing clear evidence of a slower variation only below about 2 K, and sample 6 varies more rapidly than T^3 from 4 K down to about 2.5 K, below which it begins to slow down toward T^2. These systematic differences must be accommodated by any model for the behavior of the data.

The behavior shown in Figs. 7 and 8 is completely inconsistent with the approximately T^5 variation predicted by the theorists for $4.2\ \text{K} \geq T \geq T_c$ based upon their calculations of the magni-

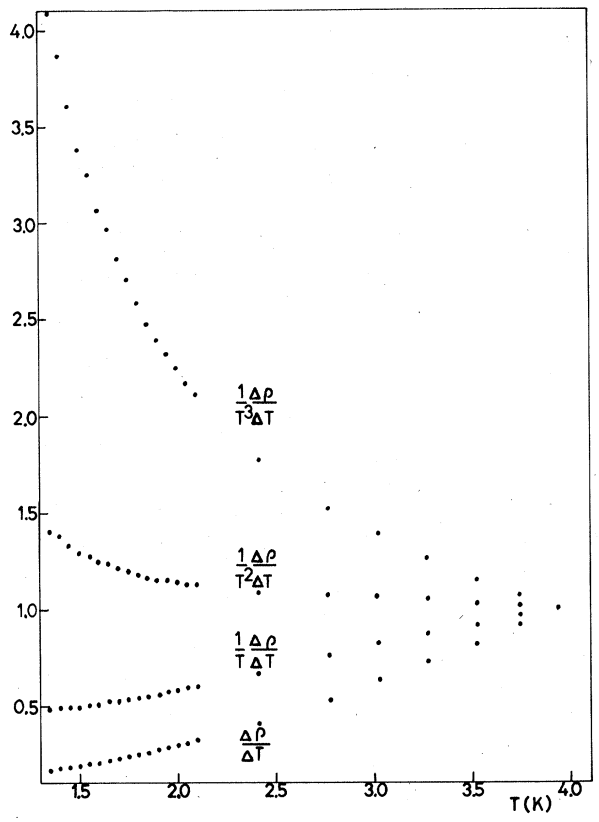

FIG. 7. Plot of $(1/T^m)$ $(d\rho/dT)$ vs T for sample 1 with $m = 0, 1, 2, 3$. To facilitate intercomparison, the data have been normalized to the value 1.00 at the highest temperature shown. Note that the mean scatter in the data is about ±1%, in accord with the analysis of uncertainties given in Sec. III.

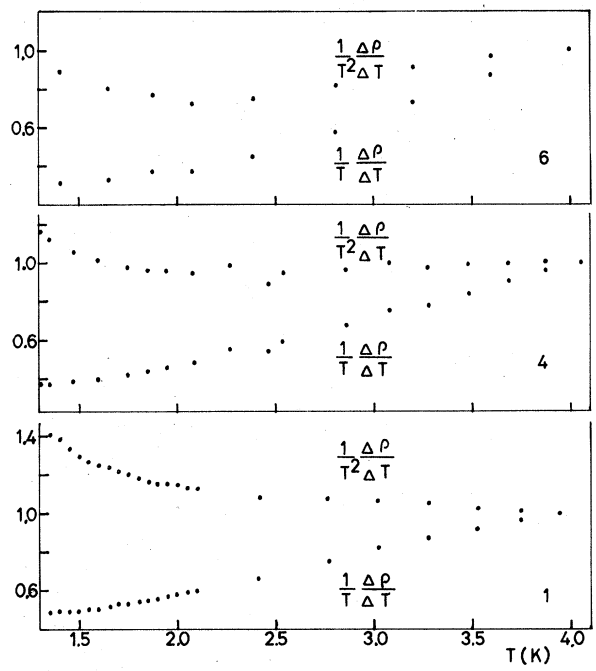

FIG. 8. Plot of $(1/T^m)(d\rho/dT)$ vs T for samples 1, 4, and 6, with $m = 1$ and 2. For each sample, the data have been normalized to the value 1.00 at the highest temperature shown. For sample 4, the derivatives have been calculated using only data points taken during a single measuring series (see Sec. III D).

tudes of $\rho_{e\text{-}ph}$ and $\rho_{e\text{-}e}$. We are therefore faced with a choice; either one or both of these calculations is wrong or there is a third mechanism at work. We examine these alternatives in parts C, D, and E.

The behavior shown in Figs. 7 and 8 is also at variance with the simple T^2 or T^3 variations reported by previous investigators. When we compare our data with theirs, we find that there are no major differences in magnitude at a given temperature. For the reported T^3 variations which were for impure samples, the differences in the conclusions drawn from the data can easily be attributed to greater scatter in their low-temperature data than in ours, especially when this greater scatter is combined with a method of analysis [plotting $\rho(T)$ versus T^3] which discriminates against just those low-temperature data points which in our measurements show the greatest deviations from a T^3 variation. For the reported T^2 variations, which were for purer samples, their larger scatter, combined with the somewhat slower than T^3 variation which we find for purer samples (see Fig. 7), can explain most of the disagreement between the conclusions reached. However, there appear to be small residual differences, especially at the lowest temperatures, which cannot be so explained. Perhaps they result from a small systematic error in their measurements due to a superconducting proximity effect arising from their use of Pb bands around their samples at the places where the potential leads were attached.[35]

C. Analysis in terms of $\rho_{e\text{-}e}$ plus a simple $\rho_{e\text{-}ph}$

1. Qualitative analysis

Since our data are not consistent with theoretical predictions, we must consider a variety of alternative ways of understanding what we see. We begin with the most conservative assumption, that the calculations of both $\rho_{e\text{-}e}$ and $\rho_{e\text{-}ph}$ are correct concerning their temperature variations, but that one or both may be in error as to magnitude.

In such a case, $\rho(T)$ should consist at the lowest temperatures of a term $\rho_{e\text{-}e} = AT^2$ and a term $\rho_{e\text{-}ph} = BT^5$. We can test for consistency of our data with this expectation by plotting $(1/T)(\Delta\rho/\Delta T)$ as a function of T^3. Such a plot should yield for each sample a straight line with slope of $5B$ and intercept with the $T = 0$ K axis of $2A$:

$$(1/T)(\Delta\rho/\Delta T) = 2A + 5BT^3 . \qquad (6)$$

In addition, to be consistent with the predictions, both coefficients must be nearly independent of ρ_0; A because electron-electron scattering is generally expected to be practically independent of ρ_0, and B because at the lowest temperatures all of the samples should be in the dirty limit.

Figure 9 shows a plot for $T < T_\lambda$ for samples 1 – 9. We see that all of the data are indeed consistent with Eq. (6). Moreover, the intercepts are all the same to within 10–15%. The slopes are also about the same to within experimental uncertainty, which however is fairly large, since the data are dominated by the coefficients A.

If this model for $\rho(T)$ is correct, then as the temperature is raised above T_λ, $\rho(T)$ should increase less rapidly than T^5, and the resistivities of the purer samples should fall below those of the less pure samples as the purer samples move out of the dirty limit. Figure 10 shows that both of these behaviors are in fact observed. In addition, since $\rho_{e\text{-}e}$ varies as T^2 over the entire temperature range, whereas $\rho_{e\text{-}ph}$ slows down to an approximately T^4 variation above T_λ, we would expect their sum to change its temperature dependence in a systematic way as the magnitude of the T^4 term increases with decreasing sample purity, falling below T^3 for purer samples in which T^2 is dominant and rising above T^3 for impure samples in which T^4 is relatively more important. The model thus provides an explanation for the systematic changes in behavior evident in Fig. 8.

2. Quantitative analysis

When we turn to quantitative analysis of the data, however, the situation becomes somewhat more

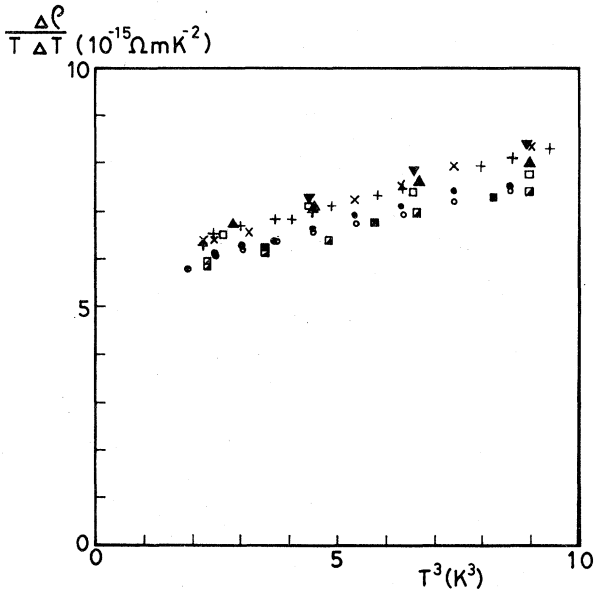

FIG. 9. $\Delta\rho/(T\Delta T)$ vs T^3 below 2.1 K for samples 1 → 9. The samples are designated by the following symbols: 1(○); 2(●); 3(+); 4(×); 5(▽); 6(▲); 7(◪); 8(■); 9(□).

complex, as we discuss in this section. We begin with alternative experimental means for estimating the magnitude of electron-electron scattering, and then turn to theoretical analyses.

a. Wiedemann-Franz ratio analysis. MacDonald *et al.*[15] have used Wiedemann-Franz ratio measurements of Powell *et al.*[36] to infer an upper bound on electron-electron scattering in Al at high temperatures. Assuming that the data are accurate to within their scatter, they obtain a bound at least three times, and perhaps an order of magnitude or more smaller than the value derived just above, depending upon the value assumed for Δ, the fractional umklapp scattering.[7] However, it is not clear to us that the data are accurate to within their scatter, in which case the bound on electron-electron scattering can be considerably larger. There is, moreover, a potential avenue for reconciling different high and low values of A: namely, electron-phonon interactions. It has recently been suggested that phonon mediation of the electron-electron interaction can produce a reduction in the coefficient A with increasing temperature,[37,38] a point which we discuss in more detail below.

Because of uncertainties in both the data and analysis, and also the possibility of a temperature variation of A, we feel that at present the Wiedemann-Franz ratio measurements do not rule out an electron-electron resistivity as large as we derive.

b. RFSE *analysis.* At low temperatures, the T^5 term in $\rho(c, T)$ due to electron-phonon scattering is expected to appear in the RFSE as a T^3 variation, while the T^2 term in $\rho(c, T)$ due to electron-electron scattering should remain as T^2. An RFSE measurement containing both components should thus display a temperature variation between T^2 and T^3. Based upon the results of comparison between RFSE and resistivity data for transition metals,[39] and upon our extrapolation of a theoretical estimate for Al,[40] an electron-electron component in $\rho(c, T)$ as large as that derived above would be expected to produce a T^2 component in the RFSE which is visible up to at least 4–6 K.

Gasparov and Harutunian[12] searched for a T^2 RFSE component in Al from 10 K down to 2 K without success. To within experimental uncertainty, their data for the single orbit studied were completely consistent with a simple T^3 variation. Some question concerning the general validity of a T^3 variation for all orbits in Al has been raised by more recent RFSE data on Al,[16] for which a variety of orbits were found to be fit better by a $T^{2.5}$ variation than by T^3. Such a variation would be compatible with a substantial electron-electron component. On the other hand, recent surface Landau level resonance (SLLR) data for Al (Ref. 41) tend to favor the T^3 variation over the $T^{2.5}$ one, although scatter in the data for most cases measured, as well as small deviations from perfect T^3 behavior, make a definitive conclusion impossible.

We have also investigated whether a comparison

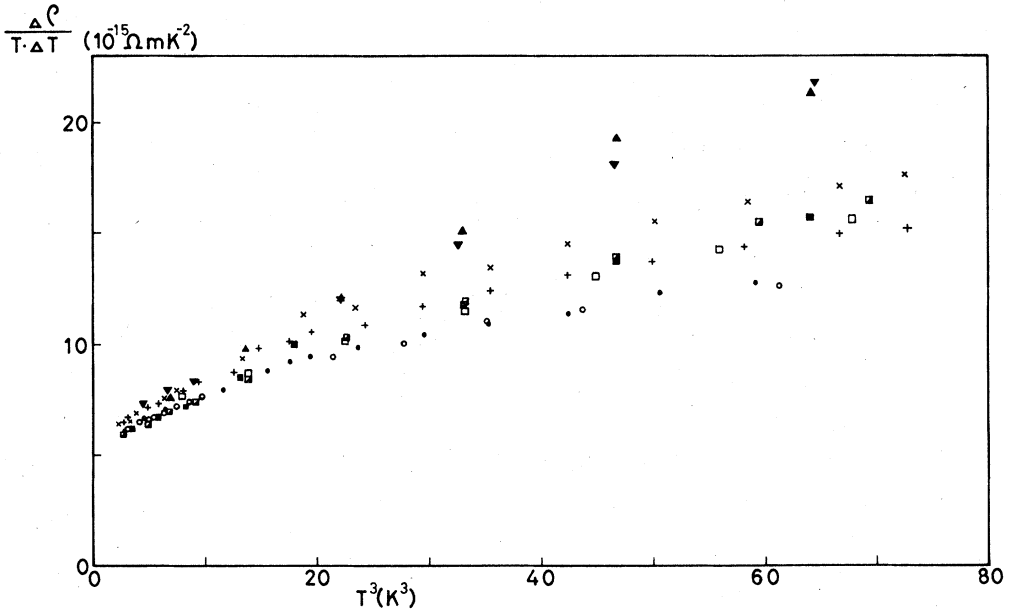

FIG. 10. $\Delta\rho/(T\Delta T)$ vs T^3 below 4.2 K for samples 1→9. For explanation of the symbols, see Fig. 9.

between observed and calculated RFSE scattering rates could provide evidence either for or against electron-electron scattering in Al. Because of variations in both experimental results and calculations for a given orbit as well as variations in the ratios of calculated to experimental rates for different orbits,[39] we decided that it could not.

We conclude that although the temperature variations in two out of three of these experiments tend to argue against as large an electron-electron component as we derive above, both additional very-low-temperature measurements and a better understanding of RFSE data analysis will be required before the RFSE data can be said to rule such a large component out. In particular, one needs to explain why such a large T^2 component in $\rho(c, T)$ is not associated with more clearly visible deviations from T^3 behavior in the RFSE data, independent of the source of the T^2 component.

3. Theory

We begin with the electron-phonon component of $\rho(c, T)$. For the coefficient B we find experimental values in the range of $4-6\times10^{-17}$ $\Omega m/K^5$, whereas the two published calculations[8,11] yield somewhat larger values of 9 and 20×10^{-17} $\Omega m/K^5$. Because the two calculations already differ from each other by a factor of two, and since such a factor is also approximately the expected reliability of each, we feel that the agreement between experiment and theory is satisfactory.

It is in the electron-electron component that the difficulty arises. Here we find coefficients A in the vicinity of 2.8×10^{-15} $\Omega m/K^2$, whereas the first detailed calculation yielded a prediction[7] of 0.12×10^{-15} $\Omega m/K^2$, more than 20 times smaller. Kaveh and Wiser[11] tentatively attributed this discrepancy to inadequate treatment of electron screening in the calculation. However, subsequent improvements in the treatment of screening[37,42] have produced little change in the predicted A for Al, which after taking into account all of the suggested improvements is still no larger than about 0.18×10^{-15} $\Omega m/K^2$.[40] It therefore seems necessary either to conclude that the T^2 component which we observe is not due to electron-electron scattering, or else to find a new mechanism to substantially increase the magnitude of the interaction between electrons in Al.

A promising suggestion for the latter has very recently been made by MacDonald[38] who pointed out that in a superconductor just above its transition temperature T_c, the attractive interaction between electrons due to phonon exchange should be larger than the repulsive screened Coulomb interaction which was the only interaction considered in the above calculations. In Al, MacDonald estimates that this attractive interaction is strongly dominant near T_c, and in combination with phonon enhancement of the quasiparticle mass, leads to an increase in the coefficient A by about the factor of 20 needed to bring experiment and theory into agreement. As the temperature rises, this attractive interaction dies away so that his model provides an explanation for the much smaller electron-electron component inferred from high-temperature Wiedemann-Franz ratio measurements[15] and perhaps also for the lack of a T^2 term in RFSE measurements,[12] on the basis that the latter measurements did not quite extend to low-enough temperatures. This last point about the RFSE, however, is only a speculation, since it is not yet known exactly how rapidly the phonon-exchange interaction decreases with temperature at the lowest temperatures. A further positive feature of MacDonald's model is that it produces little change in the coefficients A for the (non-superconducting) noble metals, where the best existing data for low-temperature electron-electron scattering[43] were already in reasonable agreement with theory.[44]

4. Concluding remarks

We see that MacDonald's calculation provides a plausible explanation for everything that has been seen in Al, including a large electron-electron component in $\rho(c, T)$ at low temperatures. On the other hand, this calculation has not yet been subject to detailed scrutiny, and previous experience suggests that further complications may yet be found. It therefore seems worthwhile to examine whether there are alternative possible interpretations of our experimental data.

D. Alternatives to electron-electron and electron-phonon scattering

In addition to being scattered by phonons and by other electrons, the electrons in a metal can also be scattered by substitutional impurities, interstitial impurities (primarily dissolved gases), the sample surface, grain boundaries, and dislocations. If any one of these scatterers were the source of $\rho(c, T)$, then a change in its concentration should produce a corresponding change in $\rho(c, T)$. Since below T_λ, $\rho(c, T)$ is dominated by its T^2 component, it suffices to examine whether changing any of the quantities of interest changes the magnitude of this component.

As is shown in Fig. 11 (see also Table I), the values of A were very nearly the same for all of our samples. We can therefore rule out as the source of A any quantity which changed significantly from sample to sample. We now list and briefly

discuss each of the quantities of interest which we are able to rule out.

(1) *Sample surface*: Samples 1 and 2 were of comparable purity, but differed in diameter by a factor of 2. In sample 1, we estimate that surface scattering produced more than half of the residual resistivity ρ_0,[21] while in sample 5 such scattering could not have produced even 1% of ρ_0. Since A was nearly the same for samples 1, 2, and 5, we can rule out temperature-dependent surface scattering (size effects)[17] as the source of A.

(2) *Grain boundaries*: In samples 2, 4, 7, and 8, the grain sizes were comparable to the diameters of the samples. In sample 2 we estimate grain boundary scattering to have produced at least 10% of ρ_0.[21] In contrast, in samples 5, 6, and 9 the grains were much smaller than the sample diameters. In all cases, the electron mean free path was smaller than the grain size. The lack of correlation between the grain size and A allows temperature-dependent grain boundary scattering[21] to be ruled out.

(3) *Dislocations*: The number of dislocations was high in the unannealed sample 9 [about 10^{14} lines/m^2 estimated from the increase in ρ_0 relative to samples 7 and 8 (Ref. 21)], but much smaller in the other samples ($\leq 10^{10}$ lines/m^2),[21] all of which were well annealed. Temperature-dependent dislocation scattering can thus also be ruled out.

(4) *Interstitial gases*: The concentrations of any dissolved interstitial gases must have been very different in samples 7, 8, and 9 which were annealed in air, in H_2, and left unannealed, respectively. Temperature-dependent scattering from interstitial gases can thus be ruled out.

(5) *Substitutional impurities*: ρ_0 varied by more than a factor of 160 with a resulting change in A of $\lesssim 10\%$. Effects due to substitutional impurities such as inelastic impurity scattering[45,17] can thus be ruled out.

(6) *Magnetoresistance*: Finally, we checked that reducing the measuring current and shielding the sample with Pb and μ metal produced little or no change in A. Magnetoresistance due to either the self-field of the sample current or to the earth's field can thus be ruled out too.

The arguments that $\rho_{e\text{-}e}$ must vary as T^2 are very general.[46] Moreover, if we are prepared to allow $\rho_{e\text{-}e}$ to be large enough to dominate $\rho(c, T)$ below T_λ, then there is no need to go beyond the analysis of Sec. IV C. The only alternative thus seems to be the possibility that below T_λ the temperature variation of $\rho_{e\text{-}ph}$ is completely different from prediction in a fashion which allows it to dominate $\rho(c, T)$ down to the lowest temperatures.

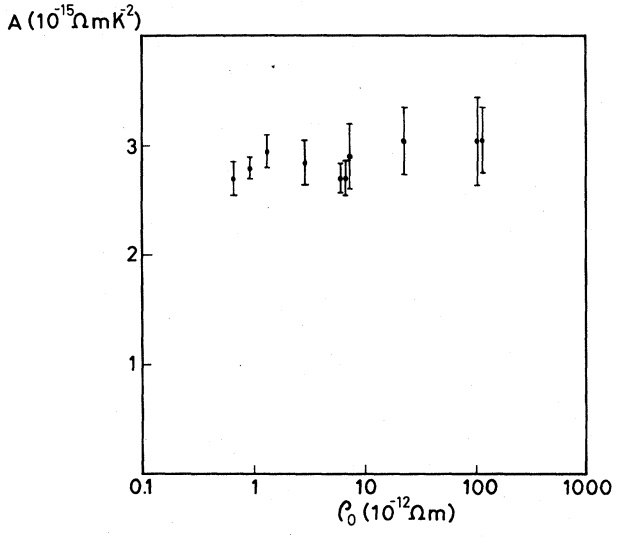

FIG. 11. The coefficient A of the T^2 term in the resistivity plotted versus the residual resistivity ρ_0. All data are consistent, within uncertainties, with $A = 2.8 \times 10^{-5}$ Ωm.

E. The effect of alternative forms for $\rho_{e\text{-}ph}(T)$ upon the size of $\rho_{e\text{-}e}(T)$

The difficulty in analyzing the data in such a case is that we have no theoretical guidance as to how to proceed. If we require electron-electron scattering to be completely negligible, then $\rho_{e\text{-}ph}(T)$ must vary at the lowest temperatures approximately as T^2, as indicated in Figs. 7 and 8. Alternatively, we can retain $\rho_{e\text{-}e} = AT^2$ as an unknown quantity and determine its magnitude experimentally for various assumed forms for $\rho_{e\text{-}ph}(T)$.

For example, if we assume that below T_λ, $\rho_{e\text{-}ph}(T)$ varies as some other power of T than T^5, then we can test whether the data are consistent with such a variation by plotting $\Delta\rho/T\Delta T$ vs T^{n-2} and looking for straight-line behavior. Figure 12 shows such a plot for the sample for which the data are most reliable, sample 1, with $n = 5$, 4, and 3. We see that, as already established in Fig. 9, the data are consistent with a straight line for $n = 5$ with a value of $A = 2.8 \times 10^{-15}$ Ωm/K^2. The data are also approximately consistent with $n = 4$, for which the derived value of A is about 10% lower. The data are, however, not consistent with $n = 3$.

If we make similar plots for the three other samples (2–4) for which the data are accurate enough to distinguish alternative possible values for n in such a fashion, then we find that samples 3 and 4 show behavior like that of sample 1, while for sample 2 a value of $n = 3$ fits the data slightly better than does $n = 5$. The difference between

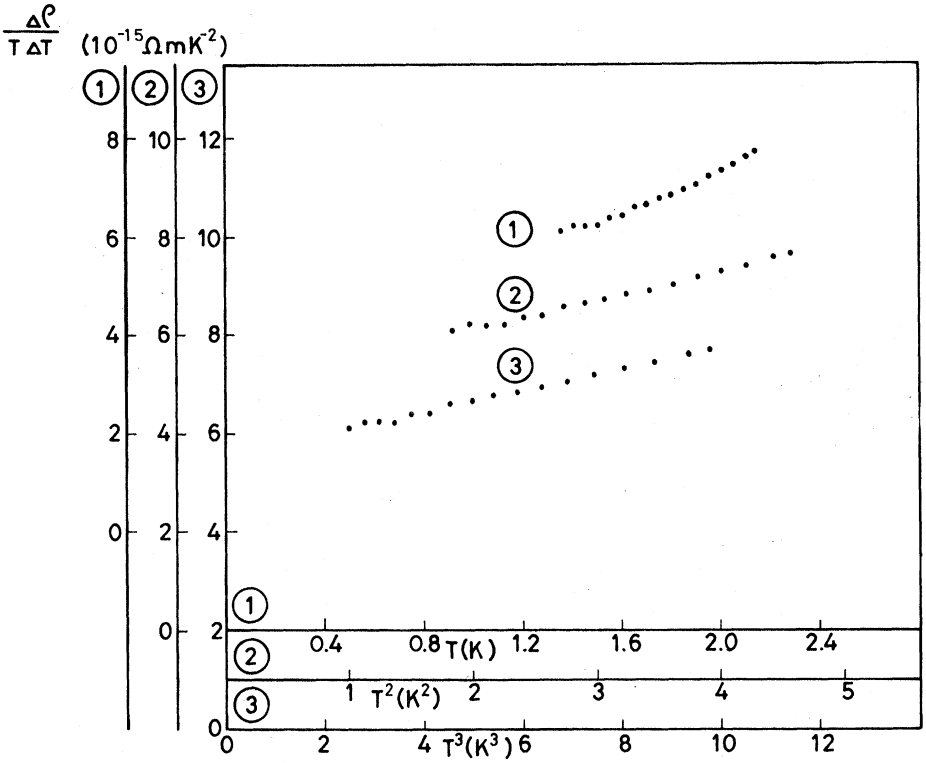

FIG. 12. $\Delta\rho/(T\Delta T)$ vs T, T^2, and T^3 for sample 1.

this sample and the other three is illustrated in Fig. 13.

We see from these two figures that allowing

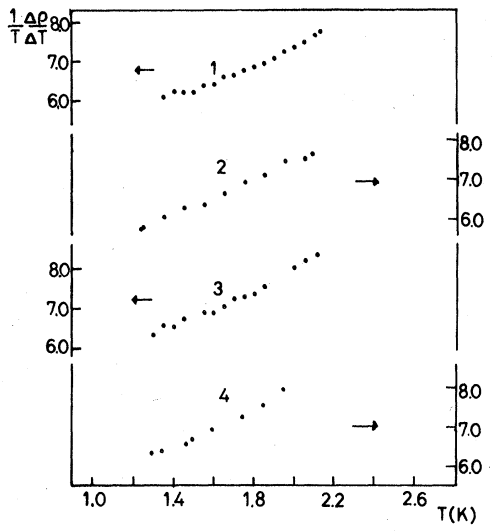

FIG. 13. $\Delta\rho/(T\Delta T)$ vs T for samples 1–4. For samples 3 and 4, the derivatives have been calculated using only data points taken during a single measuring series (see Sec. III D).

$\rho_{e\text{-}ph}$ to vary as T^4 below T_λ produces little change in A, which is reduced by only about 10%. Assuming a power of T greater than T^5 also produces little change. Requiring $\rho_{e\text{-}ph}$ to vary as T^3 would decrease A by nearly 40% if we force a straight-line fit to the data, but such a fit is inconsistent with the data for three of the four samples. In any case, we cannot reduce the electron-electron coefficient A by more than half using any integer power of T for the electron-phonon term except T^2.

In order to get a feeling for what happens with more exotic alternatives, we also examined whether the data for samples 1–4 were consistent with the form $\rho(c,T)=AT^2+Be^{-\theta/T}$. The data were indeed consistent with this formula for each sample, not only below T_λ but also up to 4.2 K. However, the parameter θ varied substantially from sample to sample, which is not what would be expected if the exponential term correctly described electron-phonon scattering in the dirty limit. Moreover, this alternative form for $\rho_{e\text{-}ph}$ had little effect on the value of A since the values found did not differ by more than about 15% from those given in Table I.

We conclude from these analyses that the only way to greatly reduce the inferred electron-elec-

tron coefficient A is for ρ_{e-ph} to vary below T_λ more slowly than T^3. Based upon existing theoretical analyses[7,11,40] it is very difficult to see how this could come about.

For those who wish to examine effects on our data of additional analyses, we list in the Appendix the resistivities for all nine of the samples for which we took careful data to well below T_λ. In order to provide the data of highest accuracy for each sample, we have included only data for the highest measuring current used in each case and omitted a few data points which for various reasons were deemed less reliable. As indicated in Sec. III B, the data for lower currents were always consistent with those given, to within the larger uncertainties associated with the lower current measurements.

F. $\rho(c,T)$ as a function of ρ_0 for fixed values of T

We conclude this analysis of our data by examining the question of whether the data show saturation into a dirty limit as a function of ρ_0.

1. $T=1.87$ K

Figure 14 shows that our data do saturate into a dirty limit to within experimental uncertainty at 1.87 K. Because at such a low temperature the temperature-dependent portion of the resistivity is an extremely small fraction of the total, we have plotted the data in this figure in derivative form, so as to eliminate any uncertainty due to the unknown parameter ρ_0.

If the data of Fig. 14 are dominated by electron-electron scattering, then they are not of great interest since electron-electron scattering in Al is expected to be essentially independent of ρ_0 whether in the dirty limit or not, and variations in any small remnant electron-phonon component will be lost in the random variation in the data. On the other hand, if electron-electron scattering makes only a small contribution to these data, then they represent the first clear observation of saturation in ρ_{e-ph} for Al.

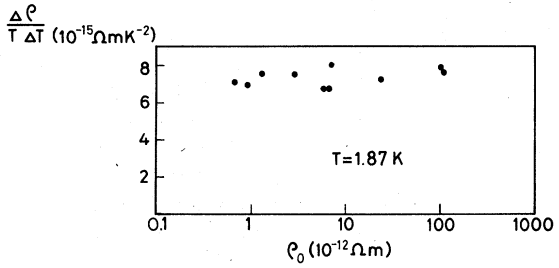

FIG. 14. $\rho/(T\Delta T)$ plotted vs ρ_0 for samples 1–9 and 12 at $T=1.87$ K.

2. $T=4.2$ K

At 4.2 K, the relative uncertainties in ρ_0 are small enough to let us make sufficiently accurate determinations of $\rho(c, 4.2\text{ K}) = \rho_t(T) - \rho_0(c)$ by a variety of extrapolation procedures. The procedure we have adopted is to define $\rho(c, 4.2\text{ K}) = \rho_t(4.2\text{ K}) - \rho_t(T_L) + AT_L^2$, where $\rho_t(4.2\text{ K})$ is the total resistivity of the sample at 4.2 K, $\rho_t(T_L)$ is the total resistivity at the lowest temperature measured on that sample, and the coefficient A is the one listed in Table I. [Where no value of A is listed, $\rho(c, 4.2\text{ K})$ was calculated using an assumed value of A identical to that of the most nearly identical sample from the table.] This procedure assumes that the sample resistivities vary as T^2 below T_L, which should be quite a good approximation at such low temperatures. The resulting values for all of our samples are listed in Table I. Figure 15 shows these values (black dots) plotted as a function of ρ_0 for all of the samples except sample 9 which was unannealed, and samples 8b and 12b, which gave points close to those for samples 8 and 12, respectively. Sample 9 is omitted because cold work is known to produce contributions to $\rho(c, T)$ in Al which at 4 K and above, differ substantially from those due to impurities.[47] Figure 15 also contains all of the data from other publications which appeared to be of sufficient accuracy to warrant inclusion.

When we examine the data of Fig. 15 we imme-

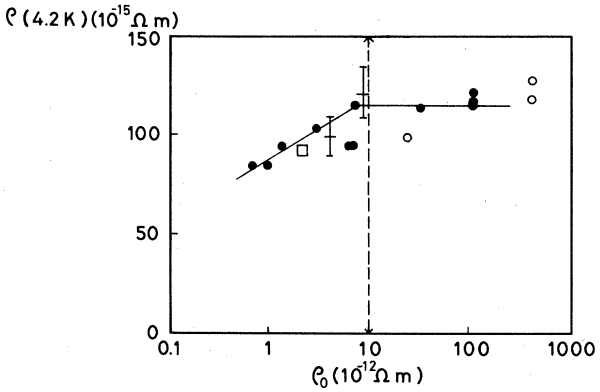

FIG. 15. The temperature-dependent part of the resistivity at 4.2 K, $\rho(c, 4.2\text{ K})$, plotted versus the residual resistivity ρ_0. The filled circles represent all the samples described in this paper except the unannealed sample 9 and samples 8b and 12b (see text). The other data come from references ○ (Ref. 9); □ (Ref. 13); and +: (Ref. 48). The vertical dashed line indicates the approximate value of ρ_0 at which the generalized two-band model would predict the onset of saturation in $\rho(c, 4.2\text{ K})$. The solid lines were drawn through the data points of the eight samples which were annealed with our standard annealing procedure, to show that these data points are compatible with saturation.

diately find a difficulty. Although the uncertainty in our determination of $\rho(c, 4.2\ \mathrm{K})$ for each sample is only about the size of one of the black dots, the data do not fall on a single curve to within the sizes of these dots. The data are thus not a unique function of ρ_0.

If we weight all of the data equally, then they determine a straight line which rises from the data points at the lower left to those at the upper right. However, the variation of the data in the middle is then as large as the entire change from one end to the other.

If, alternatively, we try to stay within the sizes of the black dots, then we find that eight of the eleven points fall on the two straight lines shown, and these are just the eight wires which were given the standard hydrogen annealing treatment of 1 h at approximately 773 K. The high point at the upper right comes from sample 11, which was annealed in air, and the two low points near $\rho_0 = 10^{-11}\ \Omega\mathrm{m}$ come from sample 7 which was also annealed in air, and from sample 8 which was annealed in hydrogen for 22 h at 773 K. Since sample 11 came from the same roll of wire as sample 5, and samples 7 and 8 came from the same plate as sample 12, it would seem that the observed differences in $\rho(c, 4.2\ \mathrm{K})$ must be due to physical differences resulting from the different annealing procedures. The pattern of differences is, however, not a simple one since air annealing raised $\rho(c, 4.2\ \mathrm{K})$ for sample 11 slightly above that for sample 4, but lowered sample 7 substantially below sample 12, and extended hydrogen annealing produced the same effect in sample 8 as air annealing did in sample 7. Moreover, all of these changes were associated with only very small changes in ρ_0. Clearly, further work is needed to establish the source, or sources, of the observed differences. If we examine the data in Fig. 15 taken by other investigators, we find that it follows the pattern of ours; five of the six samples fall near the two straight lines on the graph, while the sixth falls well below the others.

We conclude that, depending upon one's predilection, the data can be interpreted either as evidence for nonsaturation with a lot of scatter between data points, or as evidence for saturation above about $\rho_0 \approx 1 \times 10^{-11}\ \Omega\mathrm{m}$, with a few anomalous points. In the latter picture, the onset of saturation occurs when $\rho_0(c) \approx 10^2 \rho(c, 4.2\ \mathrm{K})$, which is about where it would be expected from published calculations.[19]

Finally, in Fig. 15 we have not subtracted any presumed electron-electron components from our resistivities in order that our data could be directly compared with data from other sources where the magnitudes of any AT^2 terms are not known. If instead we subtract from the $\rho(c, 4.2\ \mathrm{K})$ for each of our samples the value of $A(4.2\ \mathrm{K})^2$ appropriate to that sample, then the resulting data points are all approximately half as large as those shown in Fig. 15, but the qualitative behavior of the data remains unchanged. Thus, our analysis of saturation at 4.2 K does not depend upon whether or not we correct for electron-electron scattering.

V. SUMMARY AND CONCLUSIONS

We have measured the electrical resistivities of aluminum samples having resistance ratios ranging from 245 to 40 600, over the temperature range 4.2 to 1.8 K. In the vicinity of 4 K, the temperature-dependent portion of the resistivity, $\rho(c, T)$, varied nearly as T^3, although the actual variation was slightly slower than T^3 for the purest samples and slightly faster for the least pure ones. As the temperature was reduced, the variation became slower for all samples, approaching T^2 as $T \to 1.18$ K. At the lowest temperatures the data for all of the samples were the same to within 10–15%, thereby exhibiting saturation in $\rho(c, T)$ as a function of $\rho_0(c)$. As the temperature increased toward 4 K, systematic differences appeared, with the data for the purest samples falling below those for the less pure ones. Because of variation at 4.2 K between data for similar samples subjected to different annealing procedures, it was not possible to establish unambiguously the existence of saturation at this temperature; however, all of the data for samples given our standard hydrogen anneal were consistent with saturation for $\rho_0(c) \geq 10^{-11}\ \Omega\mathrm{m}$.

To investigate whether $\rho(c, T)$ might be influenced by sources other than electron-electron and electron-phonon scattering, various parameters such as impurity content, sample thickness, grain size, and annealing procedure were varied. At the lowest temperatures none of these parameters made any significant difference in $\rho(c, T)$, with the largest change being approximately 10% due to cold work. We conclude that at these temperatures $\rho(c, T)$ is determined almost completely by electron-electron and electron-phonon scattering. In the vicinity of 4 K, cold work and different annealing procedures produced changes up to 30–40% in $\rho(c, T)$, leaving the possibility that in this temperature range additional scattering sources such as dislocations must be considered in a complete description of what is observed.

Below T_λ, electron-phonon scattering in Al has been predicted to vary as T^5, and electron-electron scattering is expected to vary as T^2 at all temperatures in the present range of interest. We therefore tested whether the lowest-temperature data were consistent with the form $\rho(c, T) = AT^2$

$+BT^5$. They were, yielding coefficients A and B which had the same values to within experimental uncertainties for all of the samples studied. The coefficients A varied from $2.7-3.0\times10^{-15}$ $\Omega m/K^2$, with the single value 2.8×10^{-15} $\Omega m/K^2$ being consistent with all of the data to within uncertainties. The coefficients B ranged from $4-6\times10^{-17}$ $\Omega m/K^5$, with uncertainties of order 30%. These values for B are about half the predicted size and fall within the uncertainties of the predictions.

The values for A, on the other hand, are more than 20 times larger than predicted for electron-electron scattering that is dominated by the screened Coulomb repulsion between electrons,[7] and also considerably larger than estimates obtained from RFSE and Wiedemann-Franz ratio measurements on Al.

MacDonald has proposed a resolution to these discrepancies in terms of the phonon-mediated attractive interaction between electrons which gives rise to superconductivity in Al below T_c = 1.18 K. Just above T_c, he estimates that this interaction, combined with electron-phonon mass enhancement, leads to an increase in the calculated value of A by about the factor of 20 needed to bring the calculation into accord with the resistivity data. Moreover, since this attractive interaction falls off with increasing temperature, his proposal provides for an order-of-magnitude difference between high-temperature (Wiedemann-Franz ratio) and low-temperature (resistivity) values for the magnitude of electron-electron scattering, and may even be able to encompass an apparently smaller RFSE value for electron-electron scattering on the basis that the RFSE data of primary interest did not extend to low enough temperatures.

If further analysis substantially reduces the magnitude of the enhancement which MacDonald derives, then it will be very difficult to see how to bring theory and experiment into agreement. On the other hand, if his results are confirmed by such analysis, then we believe that it will be fair to conclude that there are no longer any major discrepancies between theory and experiment for the low-temperature electrical resistivity of Al.

ACKNOWLEDGMENTS

The authors would like to thank G. J. C. L. Bruls for assistance with some of the measurements, A. D. Caplin for helpful suggestions and a critical reading of the manuscript, W. E. Lawrence and M. Keveh for helpful suggestions, A. H. MacDonald, J. G. Cook, R. Taylor, and M. J. Laubitz for bringing the high-temperature Wiedemann-Franz analysis to our attention and discussing it with us by letters, and A. H. MacDonald for communicating his analysis of phonon-mediated electron-electron scattering to us prior to publication. J. Bass would also like to thank the University of Nijmegen for its kind hospitality during a portion of his sabbatical leave from Michigan State University, and to acknowledge a Science Research Council, Senior Visiting Fellowship at Imperial College, London where portions of the last drafts of this paper were completed. Part of this work has been supported by the "Stichting voor Fundamenteel Onderzoek der Materie" (FOM) with financial support of the "Nederlandse Organisatie voor Zuiver Wetenschappelijk Onderzoek" (ZWO).

APPENDIX: TABLES OF THE RAW DATA OF THE RESISTIVITY OF ALUMINUM

Values of the resistivities of nine aluminum samples as a function of temperature. The absolute accuracy for the temperature is 2 mK and for the resistivity 1%. The relative accuracies for the resistivities for the different samples are given in Table I.

Samples 1–4 were each measured over a period of several days to two weeks, during which times the sample sometimes rose to liquid-nitrogen temperature and in one case to room temperature. Although corrections were made for changes in sample parameters, using the resistances of the samples at a fixed temperature just below T_λ as a reference, these corrections sometimes still left residual differences in $\Delta\rho$ on the scale of parts in 10^5 at temperatures other than T_λ. For precision determinations of temperature derivatives of sample resistivities, we therefore recommend using only data points taken during a single series of measurements. These different series are distinguished for each sample by letters to the left of the measured temperature.

Sample 1 is the following:

T(K)	$\rho(10^{-12}\ \Omega m)$	T(K)	$\rho(10^{-12}\ \Omega m)$
b 1.298	0.933 056 5	a 2.0000	0.940 732 0
b 1.302	0.933 079 6	a 2.0500	0.941 479 5
b 1.322	0.933 241 9	a 2.0500	0.941 479 5
b 1.355	0.933 506 4	a 2.1000	0.942 259 4
b 1.362	0.933 564 3	a 2.1447	0.942 992 4
b 1.363	0.933581 9	a 2.1557	0.943 175 3
b 1.402	0.933 903 7	a 2.1666	0.943 360 8
b 1.453	0.934 358 3	a 2.1699	0.943 413 8
b 1.5003	0.934 789 4	a 2.1709	0.943 428 8
b 1.5497	0.935 260 8	c 2.1709	0.943 406 2
b 1.5500	0.935 263 5	b 2.1709	0.943 412 3
c 1.6000	0.935 767 6	b 2.647	0.953 038
a 1.6001	0.935 775 4	b 2.647	0.952 971
a 1.6502	0.936 309 0	b 2.905	0.959 818

a 1.7001	0.936 862 5	b 3.149	0.967 489
a 1.7551	0.937 499 1	b 3.401	0.976 600
a 1.7999	0.938 042 5	b 3.646	0.986 609
a 1.8500	0.938 671 1	b 3.842	0.995 565
a 1.9036	0.939 373 8	b 4.042	1.005 563
a 1.9501	0.940 012 6	b 4.106	1.009 198

Sample 2 is as follows:

T(K)	$\rho(10^{-12}\ \Omega m)$	T(K)	$\rho(10^{-12}\ \Omega m)$
d 1.180	0.671 472 0	b 2.582	0.690 981 1
d 1.191	0.671 541 7	a 2.631	0.692 153 4
d 1.225	0.671 757 1	b 2.728	0.694 563 0
d 1.298	0.672 313 4	b 2.989	0.701 856 8
d 1.401	0.673 157 1	b 3.1875	0.708 190 5
d 1.4998	0.674 059 4	b 3.3785	0.715 011 1
d 1.6012	0.675 060 4	b 3.596	0.723 428 5
d 1.7009	0.676 155 9	a 3.796	0.732 586
d 1.8009	0.677 369 1	b 3.797	0.733 019 1
d 1.9007	0.678 683 8	b 3.997	0.741 948 04
d 2.0006	0.680 138 9	c 4.1345	0.748 373 65
d 2.1006	0.681 681 6	a 4.221	0.754 193 04
d 2.1716	0.682 863 1	c 4.224	0.753 803 87
b 2.362	0.686 244 1		

Sample 3 is as follows:

T(K)	$\rho(10^{-12}\ \Omega m)$	T(K)	$\rho(10^{-12}\ \Omega m)$
d 1.253	1.305 656	b 2.0498	1.315 100
d 1.289	1.305 927	b 2.1005	1.315 964
c 1.292	1.305 974	b 2.1708	1.317 224
d 1.352	1.306 468	b 2.329	1.320 021
c 1.402	1.306 943	b 2.468	1.323 249
d 1.451	1.307 370	a 2.578	1.326 050
c 1.5013	1.307 909	a 2.725	1.330 024
c 1.5410	1.308 320	b 2.800	1.332 328
c 1.6008	1.308 967	a 2.9865	1.338 192
c 1.6503	1.309 512	a 3.186	1.345 396
c 1.7005	1.310 120	a 3.3777	1.353 208
c 1.7502	1.310 733	a 3.5955	1.363 165
c 1.8001	1.311 381	a 3.7701	1.371 986
c 1.8502	1.312 057	a 3.978	1.383 562
c 1.9001	1.312 767	a 4.1316	1.392 924
b 1.9500	1.313 510	a 4.220	1.398 541
b 2.0000	1.314 293		

Samples 4–6 are as follows:

T(K)	$\rho(10^{-12}\ \Omega m)$	T(K)	$\rho(10^{-12}\ \Omega m)$
e 1.254	2.924 621	c 2.360	2.940 252
e 1.302	2.925 007	c 2.578	2.945 254
e 1.353	2.925 446	c 2.726	2.949 722
e 1.402	2.925 872	c 2.988	2.958 420
c 1.501	2.926 785	b 3.183	2.966 233
e 1.541	2.927 216	c 3.380	2.974 923
e 1.601	2.927 868	b 3.593	2.985 701
c 1.700	2.928 991	b 3.785	2.996 700
c 1.800	2.930 262	b 3.978	3.009 021
c 1.900	2.931 660	d 4.132	3.019 693
c 2.000	2.933 214	b 4.133	3.019 844
a 2.0495	2.934 108	d 4.209	3.025 395
a 2.0999	2.934 926	c 4.221	3.026 403
c 2.1708	2.936 200		

T(K)	$\rho(10^{-12}\ \Omega m)$	T(K)	$\rho(10^{-12}\ \Omega m)$
1.522	106.801 50	1.2935	110.6396
1.763	106.804 40	1.535	110.6419
1.986	106.680 77	1.774	110.6447
2.162	106.810 82	1.990	110.647 85
2.610	106.8212	2.167	110.6508
2.994	106.8344	2.611	110.6610
3.389	106.8527	3.011	110.6748
3.389	106.8524	3.400	110.6943
3.800	106.8791	3.800	110.7211
4.218	106.9155	4.200	110.7553

Samples 7–9 are as follows:

T(K)	$\rho(10^{-12}\ \Omega m)$	T(K)	$\rho(10^{-12}\ \Omega m)$
1.224	6.628 200	1.371	6.009 10
1.224	6.628 16	1.663	6.011 85
1.433	6.629 82	1.931	6.015 10
1.600	6.631 375	2.102	6.017 61
1.773	6.633 23	2.613	6.027 68
1.989	6.636 07	3.022	6.039 22
2.167	6.638 84	3.395	6.053 42
2.628	6.648 14	3.803	6.073 69
3.019	6.659 43	4.193	6.098 09
3.4065	6.674 22	4.229	6.099 51
3.793	6.693 46		
4.101	6.706 58		
4.206	6.719 78		

T(K)	$\rho(10^{-12}\ \Omega m)$
1.241	22.449 24
1.521	22.451 75
1.762	22.454 56
1.982	22.457 62
2.166	22.460 60
2.620	22.470 02
3.016	22.481 36
3.402	22.495 58
3.699	22.509 33
3.945	22.522 75
4.211	22.539 66

*Present address: Technical Faculty, University of Suriname, Leysweg, Paramaribo, Suriname.
†Permanent address: Physics Department, Michigan State University, East Lansing, Michigan 48824.

[1]N. W. Ashcroft, Philos. Mag. 8, 2055 (1963).
[2]A. D. Caplin and C. Rizzuto, J. Phys. C 3, L117 (1970).
[3]C. Kittel, *Introduction to Solid State Physics* (Wiley, New York, 1967), 5th ed., 126.
[4]W. B. Willot, Philos. Mag. 16, 691 (1967).
[5]G. Kh. Panova, A. P. Zhernov, and V. I. Kutaitsev, Zh. Eksp. Teor. Fiz. 56, 104 (1969) [Sov. Phys.–JETP 29, 59 (1969)].
[6]J. C. Garland and R. Bowers, Phys. Konden. Mater. 9, 36 (1969).
[7]W. E. Lawrence and J. W. Wilkins, Phys. Rev. B 7, 2317 (1973).
[8]W. E. Lawrence and J. W. Wilkins, Phys. Rev. B 6, 4466 (1972).
[9]S. Senoussi and I. A. Campbell, J. Phys. F 3, L19 (1973).
[10]E. Babić, R. Krsnik, and M. Ocko, J. Phys. F 6, 73 (1976).
[11]M. Kaveh and N. Wiser, Phys. Lett. 51A, 89 (1975).
[12]V. A. Gasparov and M. H. Harutunian, Solid State Commun. 19, 189 (1976).
[13]J. C. Garland and D. J. van Harlingen, J. Phys. F 8, 117 (1978).
[14]H. van Kempen, J. H. J. M. Ribot, and P. Wyder, J. Phys. (Paris) C6, 1048 (1978); J. H. J. M. Ribot, J. Bass, H. van Kempen, and P. Wyder, J. Phys. F 9, L117 (1979).
[15]A. H. MacDonald, J. G. Cook, M. J. Laubitz, and R. Taylor (private communication).
[16]D. Parsons and C. A. Steele, J. Phys. F 9, 1783 (1979).
[17]J. Bass, Adv. Phys. 21, 431 (1972).
[18]M. R. Cimberle, G. Bobel, and C. Rizzuto, Adv. Phys. 23, 639 (1974).
[19]Y. Bergman, M. Kaveh, and N. Wiser, Phys. Rev. Lett. 32, 606 (1974).
[20]Alusol 45D from Multicore solders, Hempstead, England.
[21]F. R. Fickett, Cryogenics 11, 349 (1971).
[22]H. van Kempen, H. W. Neyenhuisen, and J. H. J. M. Ribot, Rev. Sci. Instrum. 50, 161 (1979).
[23]D. Shoenberg, *Superconductivity* (Cambridge University Press, Cambridge, England, 1962).
[24]E. Zair, M. Sinvani, B. Levy, and A. J. Greenfield, J. Phys. (Paris) C6, 496 (1978).
[25]M. Sinvani, B. Levy, and A. J. Greenfield, Phys. Rev. Lett. 43, 1270 (1979).
[26]Lake Shore Cryotronics, Eden, New York; $\rho = 1.26$ fΩm.
[27]F. G. Brickwedde, H. van Dijk, M. Durieux, J. R. Clement, and J. K. Logan, J. Res. Nat. Bur. Stand. 64A, 1 (1960).
[28]Mensor Corporation, Houston, Texas.
[29]T. McConville, Cryogenics 9, 122 (1969).
[30]Cryocal Inc., Riviera Beach, Florida, Model CR 1000.
[31]National Bureau of Standards Model 767 superconductive thermometric fixed-point device.
[32]H. H. Plumb and G. Cataland, J. Res. Nat. Bur. Stand. 69A, 375 (1965); Metrologia 2, 127 (1966).
[33]L. M. Besley and W. R. G. Kemp, Metrologia 13, 351 (1977).
[34]The 1976 provisional 0.5 to 30 K temperature scale, Bureau International des Poids et Mesures, France; Metrologia 15, 57 and 65 (1979).
[35]R. M. Boysel, R. S. Newrock, and J. C. Garland, J. Phys. F 9, L 191 (1979).
[36]M. J. Laubitz and J. G. Cook, Phys. Rev. B 7, 2867 (1973).
[37]A. H. MacDonald and D. J. W. Geldart, J. Phys. F 10, 677 (1980).
[38]A. H. MacDonald, Phys. Rev. Lett. 44, 489 (1980).
[39]D. K. Wagner and R. Bowers, Adv. Phys. 27, 651 (1978) and references therein.
[40]W. E. Lawrence (private communication).
[41]T. Wegehaupt and R. E. Doezema, Phys. Rev. B 18, 742 (1978).
[42]C. A. Kukkonen and J. W. Wilkins, Phys. Rev. B 19, 6075 (1979).
[43]M. Khoshnevisan, W. P. Pratt, Jr., P. A. Schroeder, S. Steenwyck, and C. Uher, J. Phys. F 9, L1 (1979); M. Khoshnevisan, W. P. Pratt, Jr., P. A. Schroeder, and S. Steenwyck, Phys. Rev. B 19, 3873 (1979).
[44]J. E. Black, Can. J. Phys. 56, 708 (1978); W. E. Lawrence, Phys. Rev. B 13, 5316 (1976).
[45]P. L. Taylor, Phys. Rev. 135, A1333 (1964); Yu. Kagan and A. P. Zhernov, Zh. Eksp. Teor. Fiz. 60, 1832 (1971) [Sov. Phys.–JETP 33, 990 (1971)].
[46]L. Landau and I. Pomeranchuk, Phys. Z. Sowjetunion, 10, 649 (1936).
[47]J. A. Rowlands and S. B. Woods, J. Phys. F 8, 1929 (1978).
[48]J. W. Ekin and B. W. Maxfield, Phys. Rev. B 2, 4805 (1970).